

RESEARCH ARTICLE

An unrecognized function for COPII components in recruiting the viral replication protein BMV 1a to the perinuclear ER

Jianhui Li¹, Shai Fuchs^{2,*}, Jiantao Zhang^{1,‡}, Sebastian Wellford¹, Maya Schuldiner² and Xiaofeng Wang^{1,§}

ABSTRACT

Positive-strand RNA viruses invariably assemble their viral replication complexes (VRCs) by remodeling host intracellular membranes. How viral replication proteins are targeted to specific organelle membranes to initiate VRC assembly remains elusive. Brome mosaic virus (BMV), whose replication can be recapitulated in *Saccharomyces cerevisiae*, assembles its VRCs by invaginating the outer perinuclear endoplasmic reticulum (ER) membrane. Remarkably, BMV replication protein 1a (BMV 1a) is the only viral protein required for such membrane remodeling. We show that ER-vesicle protein of 14 kD (Erv14), a cargo receptor of coat protein complex II (COPII), interacts with BMV 1a. Moreover, the perinuclear ER localization of BMV 1a is disrupted in cells lacking *ERV14* or expressing dysfunctional COPII coat components (Sec13, Sec24 or Sec31). The requirement of Erv14 for the localization of BMV 1a is bypassed by addition of a Sec24-recognizable sorting signal to BMV 1a or by overexpressing Sec24, suggesting a coordinated effort by both Erv14 and Sec24 for the proper localization of BMV 1a. The COPII pathway is well known for being involved in protein secretion; our data suggest that a subset of COPII coat proteins have an unrecognized role in targeting proteins to the perinuclear ER membrane.

KEY WORDS: COPII, Erv14, Viral replication protein targeting, Protein perinuclear ER localization, Positive-strand RNA viruses, Viral replication complexes

INTRODUCTION

Positive-strand RNA [(+)RNA] viruses include many important human, animal and plant pathogens. All well-studied (+)RNA viruses assemble their viral replication complexes (VRCs) by remodeling host intracellular membranes, and different viruses target particular organelle membranes to initiate VRC assembly. For instance, hepatitis C virus, brome mosaic virus (BMV) and tobacco mosaic virus replicate in association with endoplasmic reticulum (ER) membranes. In contrast, Flock House virus and carnation Italian ringspot virus replicate in mitochondria, whereas tomato bushy stunt virus replicates in peroxisomes (den Boon et al., 2010; Laliberté and Sanfaçon, 2010; Paul and Bartenschlager, 2013; Romero-Brey and Bartenschlager, 2014). However, the

mechanisms by which viruses target their replication proteins to particular membranes for VRC assembly are not well documented.


BMV belongs to the plant virus family *Bromoviridae* and is a productive model for dissecting virus–host interactions and viral replication mechanisms of (+)RNA viruses (Diaz and Wang, 2014; Wang and Ahlquist, 2008). BMV genomic replication can be reconstituted in the yeast *Saccharomyces cerevisiae*, duplicating nearly all features of BMV replication in its natural plant hosts (Janda and Ahlquist, 1993; Restrepo-Hartwig and Ahlquist, 1996; Schwartz et al., 2002; Wang and Ahlquist, 2008). BMV has a tripartite RNA genome and a sub-genomic mRNA, RNA4. BMV encodes two replication proteins, BMV 1a and 2a^{pol}, which are necessary and sufficient for genomic replication in plants and yeast. BMV 2a^{pol} contains a central RNA-dependent RNA polymerase (RdRp) domain and serves as a replicase. BMV 1a contains an N-terminal RNA-capping domain (Ahola and Ahlquist, 1999; Kong et al., 1999) and a C-terminal NTPase or helicase-like domain (Wang et al., 2005). In yeast, expression of 1a and 2a^{pol}, along with other host factors, supports the replication of BMV genomic RNAs. BMV VRCs are formed by invaginating the outer perinuclear ER membrane into the ER lumen, giving rise to spherular compartments that are 60 to 80 nm in diameter with a neck-like opening of ~10 nm that connects the VRC interior to the cytoplasm (Schwartz et al., 2002). The expression of BMV 1a alone in yeast induces the formation of spherules, which are morphologically indistinguishable from VRCs. When co-expressed, BMV 2a^{pol} and genomic RNA are recruited by BMV 1a into the interior of spherules, which then become VRCs (Schwartz et al., 2002). An amphipathic α -helix within BMV 1a, helix A (amino acids 392–407), is required for its perinuclear ER membrane association in yeast and for BMV infection in plants (Liu et al., 2009). The formation of BMV-1a-induced spherules also requires host proteins (Diaz and Wang, 2014). Well-studied examples include reticulons (RTNs) and sucrose nonfermenting7 (Snf7), which are recruited by BMV 1a through protein–protein interactions and are required for spherule formation in yeast (Diaz et al., 2010, 2015). However, the mechanism by which BMV 1a is targeted to the perinuclear ER membrane is still unknown.

Coat protein complex II (COPII) is the cellular machinery responsible for anterograde protein trafficking from the ER to the Golgi. The core components of COPII include the GTPase Sar1, which initiates vesicle formation, an inner shell complex comprising Sec23 and Sec24, and an outer shell complex comprising Sec13 and Sec31 (Brandizzi and Barlowe, 2014; D’Arcangelo et al., 2013; Lord et al., 2013). Sec24 serves as the principle cargo recruiter by recognizing sorting signals present in cargos and recruiting them into vesicles. However, many cargos do not have Sec24-binding motifs and, therefore, require a cargo receptor to facilitate their incorporation into vesicles (Belden and Barlowe, 2001; Herzog et al., 2012; Kuehn et al., 1998; Miller et al., 2003; Mossessova et al., 2003; Pagant et al., 2015). As a typical cargo receptor, ER-vesicle protein of 14 kD (Erv14) binds to both its client cargos and Sec24 to

¹Department of Plant Pathology, Physiology, and Weed Science, Virginia Tech, Blacksburg, VA 24061, USA. ²Department of Molecular Genetics, Weizmann Institute of Sciences, Rehovot 7610001, Israel.

*Present address: Department of Pediatric Endocrinology and Metabolism, The Hospital for Sick Children, Toronto, Ontario, Canada M5G 1X8. [‡]Present address: Department of Pharmacology and Toxicology, The University of Arizona, Tucson, AZ 85721, USA.

[§]Author for correspondence (reachxw@vt.edu)

 X.W., 0000-0002-3850-3274

facilitate cargo incorporation into vesicles for ER exit (Herzig et al., 2012; Pagant et al., 2015; Powers and Barlowe, 2002). It has only recently been shown that COPII coat components have additional functions such as contributing to the biogenesis of autophagosomes (Davis and Ferro-Novick, 2015; Ge et al., 2014; Wang et al., 2014).

Here, we report that perinuclear ER membrane association of BMV 1a requires *Erv14*, which interacts and colocalizes with BMV 1a. Deletion of *ERV14* disrupts proper distribution of BMV 1a, leads to the formation of BMV spherules that are less abundant in number but larger in size, and significantly inhibits BMV RNA replication. We further demonstrate that the ability of *Erv14* to bind to cargos and to COPII vesicles is required for the perinuclear ER localization of BMV 1a. In addition, three COPII coat proteins, *Sec13*, *Sec24* and *Sec31*, are also required for proper BMV 1a distribution. Our data, therefore, suggest an unrecognized function for COPII components in targeting a viral replication protein to the perinuclear ER membrane, in sharp contrast to their canonical role in cargo exit from ER membranes.

RESULTS

A high-content screen identifies host factors involved in BMV 1a localization

To identify host factors that colocalize with BMV 1a and might, therefore, have a role in its recruitment to the perinuclear ER, we screened a yeast GFP (green fluorescent protein)-tagged library (Huh et al., 2003). The mCherry-tagged version of BMV 1a (BMV-1a-mC) used for the screen localized primarily at the perinuclear ER membrane (Fig. 1A, upper panels), similar to BMV 1a without a tag

(Wang et al., 2005). Using automated mating approaches (Cohen and Schuldiner, 2011), we then integrated BMV-1a-mC into the GFP-tagged library and imaged all resulting strains using a high-throughput microscopy platform (Breker et al., 2013).

Table 1 lists the 17 candidate hits identified in the screen. Among them, choline-requiring 2 (*Cho2*) has been shown to be enriched at the perinuclear ER and to colocalize with BMV 1a during BMV replication (Zhang et al., 2016), validating our approach. Three hits (*Ncw2*, *Cwp2* and *Fit2*) were discarded as they were mislocalized due to the GFP tag at the C-terminus. Interestingly, two of the hits were enzymes involved in ergosterol synthesis, *Erg3* and *Erg24* (Mo and Bard, 2005). Remarkably, eight of the hits were nuclear pore complex (NPC) proteins (*Pom33*, *Ndc1*, *Nup2*, *Nup85*, *Nup100*, *Nup145*, *Nup157* and *Nup159*), suggesting that spherules form near NPCs. Two additional hits were *Kre1* and *Gpi11*, both important for cell wall formation (Boone et al., 1991; Taron et al., 2000). The final hit, *Erv14*, posed a conundrum. As a cargo receptor, *Erv14* is known to facilitate ER exit of more than 20 cargo proteins that are membrane proteins with a long transmembrane domain (TMD) (Herzig et al., 2012; Pagant et al., 2015; Powers and Barlowe, 2002). However, in contrast to the role of *Erv14* in facilitating client cargos for ER exit, BMV 1a remains in ER membranes without evidence suggesting its exit from the ER (Schwartz et al., 2002).

Deleting *ERV14* disrupts perinuclear ER localization of BMV 1a

To assess whether any of the candidate proteins have a role in determining the localization of BMV 1a, we checked the

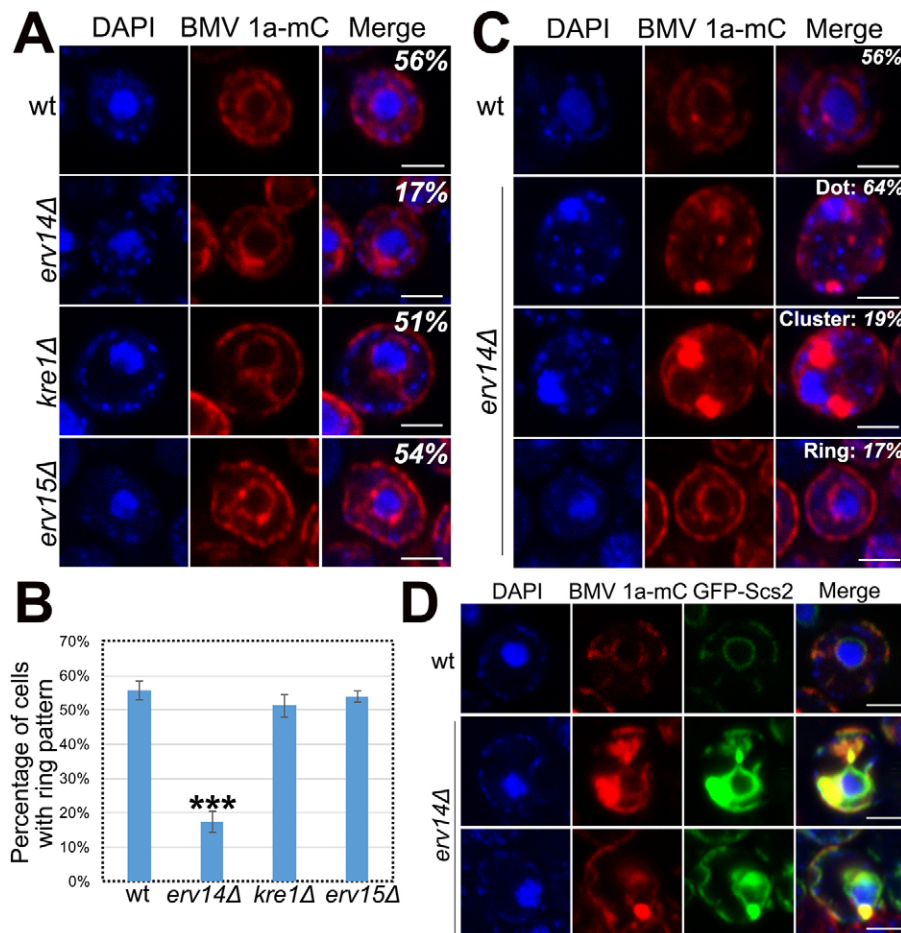


Fig. 1. Host *Erv14* is required for the perinuclear ER localization of BMV-1a-mC in yeast.

(A) Confocal microscopy images of BMV-1a-mC in wild-type (wt) or selected deletion mutant cells. The ring localization pattern, which indicates the localization of BMV 1a at the perinuclear ER membrane, was the most common (>50% cell population) in wt ($n=723$), *kre1Δ* ($n=459$) and *erv15Δ* ($n=760$) cells with BMV-1a-mC signal. The percentage of cells with the ring pattern is shown. (B) Percentage of cells with the BMV-1a-mC ring pattern in the wt, *erv14Δ*, *kre1Δ* and *erv15Δ* cells analyzed in A. Results are mean \pm s.d. *** $P<0.001$ (ANOVA single factor analysis of percentage of the deletion mutant cells with BMV-1a-mC ring localization rate as compared to that in wt). (C) BMV-1a-mC distribution in wt ($n=723$) and *erv14Δ* ($n=1255$) cells. The percentage of cells with a ring, dot or cluster localization pattern is shown. (D) Dot and cluster structures colocalize with the ER membrane marker GFP-Scs2 in *erv14Δ* cells. Nuclei were stained with DAPI (blue). Scale bars: 2 μ m.

Table 1. The hit list of yeast GFP-tagged library screening

Open reading frame	Gene name	Essential gene
YGR157W	<i>CHO2</i>	No
YLR194C	<i>NCW2</i>	No
YKL096W-A	<i>CWP2</i>	No
YOR382W	<i>FIT2</i>	No
YLR056W	<i>ERG3</i>	No
YNL280C	<i>ERG24</i>	No
YLR335W	<i>NUP2</i>	No
YJR042W	<i>NUP85</i>	Yes
YKL068W	<i>NUP100</i>	No
YGL092W	<i>NUP145</i>	Yes
YER105C	<i>NUP157</i>	No
YIL115C	<i>NUP159</i>	Yes
YLL023C	<i>POM33</i>	No
YML031W	<i>NDC1</i>	Yes
YNL322C	<i>KRE1</i>	No
YDR302W	<i>GPI11</i>	Yes
YGL054C	<i>ERV14</i>	No

localization of BMV-1a-mC by performing epifluorescence and confocal fluorescence microscopy in yeast strains lacking the individual candidate genes for those that are non-essential (Table 1). A ring localization pattern indicating perinuclear ER distribution of BMV-1a-mC was observed in ~50 to 56% of the wild-type (wt) cell population showing the mCherry signal. A similar pattern was found in many deletion mutants, as illustrated for Kre1 (Fig. 1A). Surprisingly, the ring pattern was only observed in 17% of *ERV14* deletion (*erv14Δ*) cells, a statistically significant reduction ($P < 0.001$, Fig. 1B). *ERV14* has a paralog, *ERV15*, whose deletion did not affect localization of BMV 1a (Fig. 1A,B).

Three major localization patterns of BMV-1a-mC were observed in *erv14Δ* cells: ~64% of cells had punctate dots and ~19% of cells had clusters, whereas only ~17% of cells had a ring structure (Fig. 1C). It should be noted that the percentage of each pattern varied among experiments; however, in all cases the percentage of cells with a ring pattern was significantly less than those with cluster and dot patterns. These differences might be related to the growing stage at which cells were harvested, BMV-1a-mC expression levels and/or minor differences in growth conditions, among others. To eliminate the possibility that the altered distribution was due to the addition of the mCherry tag to BMV 1a, we repeated the experiments using a Histidine6-tagged version of BMV 1a (BMV-1a-His6). About 70% of wt cells expressing BMV-1a-His6 had a ring structure in the perinuclear ER (Fig. S1). Similar to with BMV-1a-mC, in *erv14Δ* cells BMV-1a-His6 was predominantly found as dots (65%) with only 3% as clusters (Fig. S1). About 32% of *erv14Δ* cells had the ring structure, a statistically significant reduction ($P < 0.001$).

To determine the nature of the dot and cluster structures, we co-expressed BMV-1a-mC with ER, Golgi and inclusion bodies markers. The dot and cluster structures did not colocalize with the Golgi marker plasma membrane ATPase related 1 (Pmr1) (Antebi and Fink, 1992) in *erv14Δ* cells (Fig. S2, $n=100$). However, the inclusion body marker von Hippel-Lindau (VHL) protein (Kaganovich et al., 2008) colocalized with a fraction of clusters or dots in 44 out of 100 *erv14Δ* cells (Fig. S2). In contrast, the ER membrane marker suppressor of choline sensitivity 2 (Scs2) (Manford et al., 2012) associated with the majority of disrupted BMV-1a-mC structures in most *erv14Δ* cells (97 out of 100 counted cells, Fig. 1D). It should be noted that BMV-1a-mC colocalized with Scs2 primarily in the perinuclear ER membrane in wt cells (Fig. 1D, upper panels). These data suggest that deleting *ERV14*

might not affect the ER membrane association of BMV 1a but rather its enrichment to the perinuclear ER membrane.

Deleting *ERV14* affects spherule formation and genomic replication of BMV

We next examined the effects of deleting *ERV14* on BMV spherule formation and genomic replication, both of which normally occur on perinuclear ER membranes (Schwartz et al., 2002). Expression of BMV 1a in yeast induces the formation of spherules by invaginating the outer perinuclear ER membrane into the ER lumen. No spherules were found in wt and *erv14Δ* cells in the absence of BMV 1a as assessed with transmission electron microscopy (Fig. 2A). Agreeing well with prior results (Zhang et al., 2012, 2016), in wt cells there were 7.2 ± 1.6 spherules per cell section with an average diameter of 74.3 ± 24.8 nm (mean \pm s.d.; $n=122$). In *erv14Δ* cells, the average number of spherules per cell section decreased to 3.0 ± 1.3 ($n=67$). Intriguingly, we observed two spherule populations in *erv14Δ* cells, the first group had an average diameter similar to that in wt cells, whereas the diameter of the second group was larger than that of wt spherules, resulting an average size of 95.2 ± 36.1 nm, a 28% increase over those of wt (Fig. 2B).

We next measured BMV genomic RNA replication in *erv14Δ* cells expressing BMV 1a, 2a^{pol} and a genomic RNA3 transcript, all of which were expressed from plasmids. Deleting *ERV14* reduced BMV RNA replication by ~threefold (Fig. 2C) based on the accumulation of positive-strand RNA4 and negative-strand RNA3 molecules, which are only produced during BMV replication. Accumulation of BMV 1a was not significantly affected by deleting *ERV14* (Fig. 2D), eliminating the possibility that the decrease in spherule numbers and genomic replication was due to effects on BMV 1a expression and/or stability.

The perinuclear ER localization of BMV-1a-mC requires the canonical function of *Erv14*

We hypothesized that *Erv14* might simply serve as an attachment factor for BMV 1a given that *Erv14* is primarily detected at the perinuclear ER membrane (Pagant et al., 2015). Alternatively or additionally, *Erv14* might be required to facilitate the distribution of BMV 1a through its association with COPII vesicles. To verify which of the above possibilities was correct, we checked the localizations of BMV-1a-mC in *erv14Δ* cells co-expressing one of two *Erv14* mutants that retain the perinuclear ER localization but block the ability of *Erv14* to bridge cargos to COPII vesicles (Pagant et al., 2015). With three predicted TMDs, *Erv14* contains an N-terminal cytoplasmic domain, an ER lumen loop, a cytoplasmic loop and a C-terminal ER lumen tail (Fig. 3A) (Pagant et al., 2015; Powers and Barlowe, 2002). Mutations in the second TMD at amino acids 62 and 63 (*Erv14*^{62-63A}) block *Erv14* from binding to its client cargos whereas mutations in the cytoplasmic loop at amino acids 97–101 (*Erv14*^{97-101A}) prevent *Erv14* from binding to Sec24, and thus, COPII vesicles (Pagant et al., 2015; Powers and Barlowe, 2002) (Fig. 3A). As such, cargos are retained at the ER and are not transported to their final destinations. The two *Erv14* mutants were expressed under control of the endogenous promoter from a low-copy-number plasmid. In *erv14Δ* cells with an empty vector, BMV-1a-mC displayed a ring localization pattern in ~23% of cells (Fig. 3B). Expressing wt *Erv14* increased the number of cells with a normal distribution to 63%, close to a threefold increase. However, neither of the *Erv14* mutants complemented the defective distribution of BMV-1a-mC as the percentage of cells with a ring pattern was close to that in cells expressing an empty plasmid

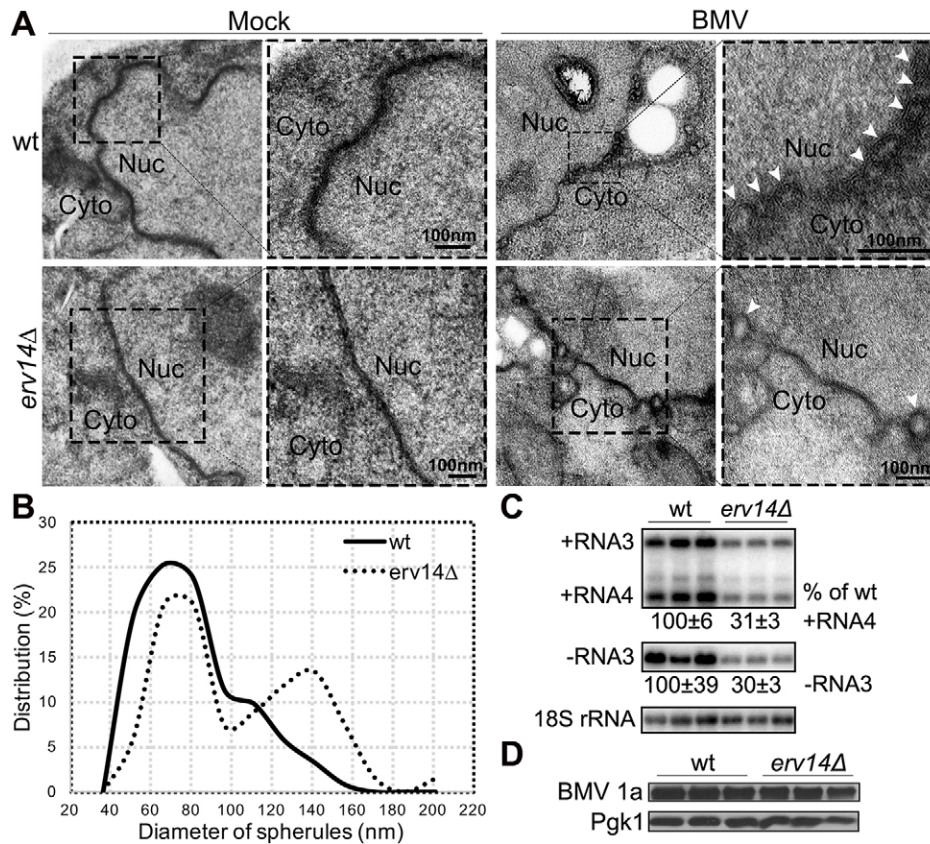


Fig. 2. Deleting *ERV14* affects the morphology of BMV spherules and inhibits BMV RNA replication. (A) Electron micrographs of wt and *erv14Δ* cells in the absence (Mock) or presence of BMV replication (BMV). Nuc, nucleus; Cyto, cytoplasm. Arrowheads point out spherules. (B) Distribution of spherule sizes in both wt and *erv14Δ* cells. Two groups of spherules with different sizes were observed in *erv14Δ* cells: the diameter of the first population was similar to that in wt cells whereas the diameter of the second population was larger. Sixty-seven spherules were examined. (C) BMV RNA replication was inhibited in *erv14Δ* cells. BMV positive- or negative-strand RNA was detected by ^{32}P -labeled BMV strand-specific probes. 18S rRNA was detected using an 18S rRNA specific probe to serve as a loading control. The values given are mean±s.d. for three experiments. (D) Accumulated BMV 1a levels in wt and *erv14Δ* cells. Anti-BMV 1a antiserum was used to detect BMV 1a. Pgk1 served as a loading control. A representative blot is shown.

(Fig. 3B). The inability of *Erv14* mutants to restore the localization of BMV-1a-mC was not due to its instability, as both accumulated to similar levels as the wt protein (Fig. 3C) (Pagant et al., 2015). These data suggest that the canonical function of *Erv14* in the COPII pathway is required for the perinuclear ER localization of BMV 1a.

BMV 1a interacts with *Erv14*

To test whether *Erv14* binds to BMV 1a and thus, whether the effect of *ERV14* deletion on the localization of BMV 1a was direct, we co-expressed a HA-tagged version of *Erv14* (*Erv14*-HA) with BMV-1a-mC in *erv14Δ* cells. *Erv14*-HA colocalized with BMV-1a-mC at the perinuclear ER in 47% of cells, a twofold increase over those

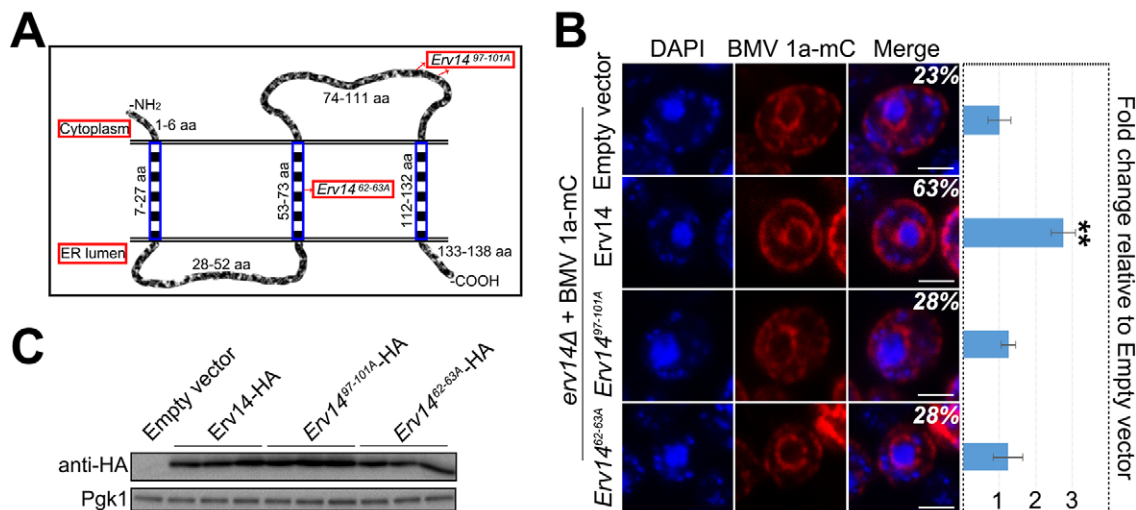


Fig. 3. BMV 1a perinuclear ER localization requires the ability of *Erv14* to bind to cargos and COPII vesicles. (A) Illustration of the predicted *Erv14* structure. The red arrows indicate mutation at amino acids 62–63 and 97–101, which block binding of *Erv14* to its client cargo and to Sec24, respectively. (B) The percentage of *erv14Δ* cells displaying the ring pattern when BMV-1a-mC was co-expressed with an empty vector ($n=717$), or with plasmids expressing HA-tagged *Erv14* ($n=682$), *Erv14*^{97-101A} ($n=683$) or *Erv14*^{62-63A} ($n=549$). Representative images of the BMV-1a-mC ring pattern are shown. Results are mean±s.d. ** $P<0.01$ (ANOVA single factor analysis as in Fig. 1). Scale bars: 2 μm . (C) Accumulated *Erv14*, *Erv14*^{97-101A} or *Erv14*^{62-63A} levels in *erv14Δ* cells. Total proteins from equal numbers of cells were separated by SDS-PAGE. *Erv14* proteins were expressed under the control of *ERV14* promoter from a centrameric plasmid and were detected using an anti-HA pAb by western blotting. Pgk1 served as a loading control. A representative blot is shown.

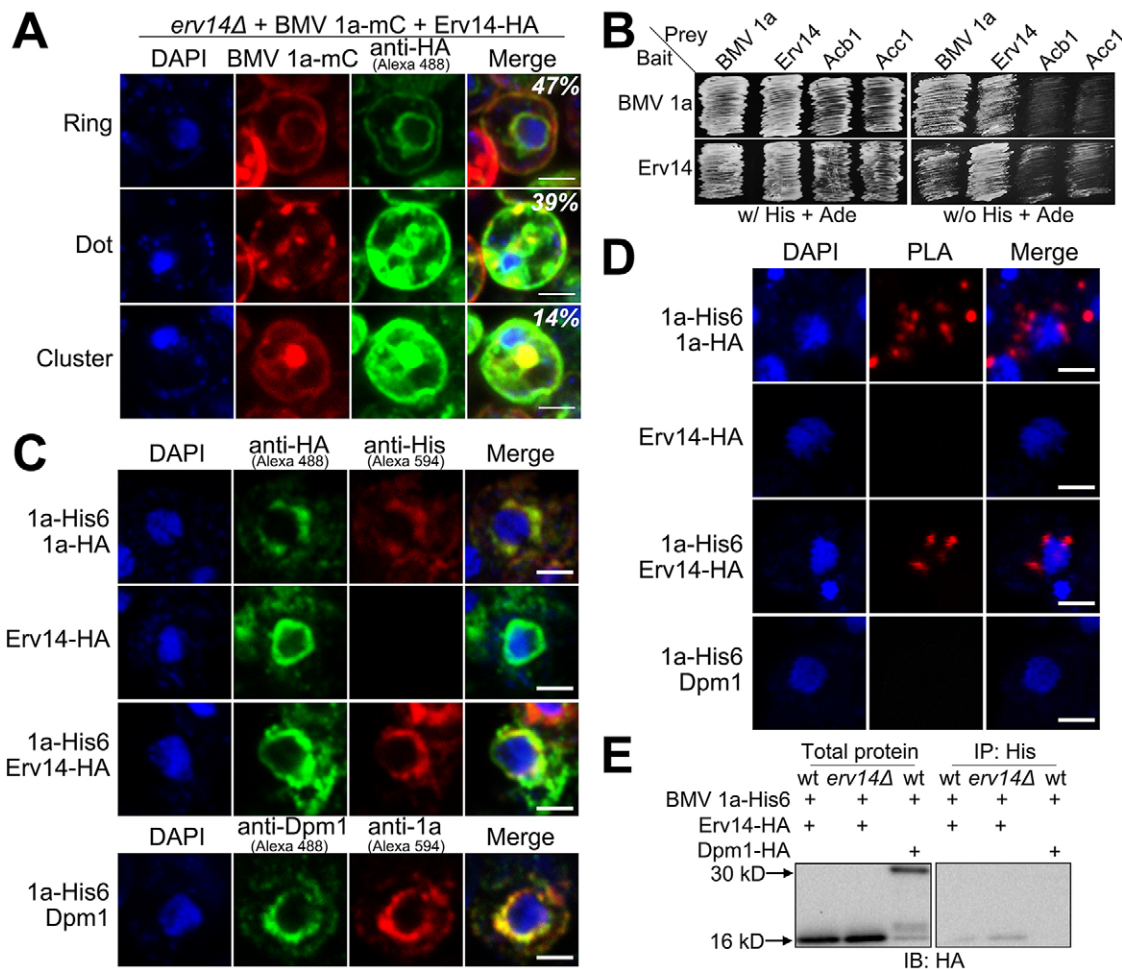


Fig. 4. BMV 1a interacts with Erv14. (A) Images of *erv14Δ* cells expressing BMV-1a-mC and Erv14-HA. The percentage of cells displaying the various BMV-1a-mC localization patterns is shown ($n=1062$). Erv14-HA was detected by using an anti-HA pAb and immunofluorescence microscopy. (B) The interaction between BMV 1a and Erv14 as assayed in the mating-based split ubiquitin system (mbSUS). BMV 1a self-interaction served as a positive control, the pairs of BMV 1a and Acb1 or Acc1 served as negative controls. Diploid cells expressing a pair of target genes were grown on medium supplemented with (w/) or without (w/o) histidine (His) and adenine (Ade). (C) Immunofluorescence images of wt cells co-expressing BMV-1a-His6 and BMV-1a-HA (top), or *erv14Δ* cells expressing Erv14-HA only (second row), or BMV-1a-His6 and Erv14-HA (third and fourth rows). BMV-1a-HA, Erv14-HA and BMV-1a-His6 were detected by using an anti-HA pAb or an anti-His mAb as primary antibodies. In the fourth row, BMV-1a-His6 and endogenous Dpm1 were detected using anti-BMV-1a antiserum and an anti-Dpm1 mAb, respectively. (D) Proximity ligation assay (PLA) signal (red) was detected using the same primary antibody combinations as in C: anti-His mAb and anti-HA pAb in cells co-expressing BMV-1a-His6 and BMV-1a-HA (positive control), or BMV-1a-His6 and Erv14-HA. Erv14-HA only or the pair of BMV-1a-His6 and Dpm1 served as negative controls. (E) Erv14-HA co-immunoprecipitates with BMV-1a-His6. Cells expressing BMV-1a-His6 and Erv14-HA or Dpm1-HA were lysed, subjected to immunoprecipitation with an anti-His (IP: His) mAb, separated by SDS-PAGE and subjected to western blotting with an anti-HA pAb (IB: HA). Dpm1-HA served as a negative control. Representative results are shown. Scale bars: 2 μ m.

with an empty vector (16%) (Fig. 4A). Interestingly, BMV-1a-mC dots were predominant when Erv14-HA failed to associate with the perinuclear ER (Fig. 4A). Although the reason for why Erv14 fails to localize to the perinuclear ER is unclear, this tight dependence again suggests a direct relationship between the two proteins.

To demonstrate that BMV 1a interacts with Erv14, we first used a mating-based split ubiquitin system (mbSUS), which detects protein-protein interactions in their native environment (Obrdlik et al., 2004). We used BMV 1a self-interaction as a positive control, as it is known to self-interact (O'Reilly et al., 1997) and form oligomers (Diaz et al., 2012). Indeed, when BMV 1a was used as bait, it interacted with itself but not with two other proteins, acyl-CoA-binding 1 (Acb1) and acetyl-coA carboxylase 1 (Acc1) (Fig. 4B). Moreover, when Erv14 served as bait, it did not interact with Acb1 and Acc1. Erv14 and BMV 1a interacted regardless of which protein was used as a bait or prey (Fig. 4B). In addition, we

found that Erv14 interacted with itself (Fig. 4B). However, the biological significance of the self-interaction of Erv14 to its cellular function and the distribution of BMV 1a is currently unknown.

To verify the BMV-1a-Erv14 interaction, we next performed an *in situ* proximity ligation assay (PLA), which we recently used to confirm the interaction between BMV 1a and the host protein Cho2 (Zhang et al., 2016). In PLA, a monoclonal antibody (mAb) and a polyclonal antibody (pAb) that recognize each component of the protein pair is incubated with fixed spheroplasts (yeast cells without cell wall). If the two proteins are close together (<30 nm), a fluorescent dye will be deposited after performing PLA (Soderberg et al., 2006). Positive PLA signals surrounding the nucleus were detected in cells expressing the BMV-1a-His6 and BMV-1a-HA pair, which served as a positive control (Fig. 4D). The pair of BMV-1a-His6 and dolichol phosphate mannose synthase 1 (Dpm1) was included as a negative control. No PLA signal was detected when

cells were incubated with anti-BMV-1a antiserum and an anti-Dpm1 mAb (to detect endogenously expressed Dpm1), even though both proteins colocalized at the perinuclear ER membrane (Fig. 4C). In addition, PLA signals were never identified in cells expressing only Erv14–HA (Fig. 4D). In cells co-expressing BMV-1a–His6 and Erv14–HA, PLA dots were observed near the nucleus when an anti-His mAb and an anti-HA pAb were used, suggesting an interaction between BMV 1a and Erv14.

We also performed a co-immunoprecipitation assay to confirm the interaction. Given that the interaction of Erv14 with its cargos, for example, axial 2 bud site selection (Axl2), is transient (Powers and Barlowe, 2002), we crosslinked samples with 1% formaldehyde and used plasmid-borne Dpm1–HA to control for non-specific crosslinking in the co-immunoprecipitation (Zhang et al., 2016). BMV-1a–His6 consistently pulled down Erv14–HA when an anti-His antibody was used in the co-immunoprecipitation assay in both wt and *erv14Δ* cells (Fig. 4E). By contrast, Dpm1–HA was not pulled down under the same conditions (Fig. 4E), verifying a specific interaction between BMV 1a and Erv14. However, we did not detect BMV-1a–His6 after crosslinking and pulling down Erv14–HA.

BMV-1a–mC behaves like an Erv14-dependent cargo

The role of Erv14 as a cargo receptor is to help recruit cargo that weakly binds to Sec24 on its own or cannot bind directly at all. Cargos with either a DxEx (x as any amino acid) or LASLE sorting

signal can bind directly to Sec24 (Mossesso et al., 2003; Votsmeier and Gallwitz, 2001). It has been shown that the addition of DLE motif to mating-pheromone-induced death 2 (Mid2), an Erv14-dependent cargo, facilitates Mid2–DLE ER exit in *erv14Δ* cells (Herzig et al., 2012). If the role of Erv14 in BMV 1a localization is mediated through COPII vesicles, its deletion should be bypassed by the addition of a sorting signal at the C-terminus of BMV-1a–mC. We, therefore, added either DLE or LASLE (Fig. 5A) to BMV-1a–mC. We also included an 8-amino-acid linker (GDGAGLIN) between BMV-1a–mC and the sorting signal to increase the accessibility of DLE or LASLE by Sec24. Addition of either DLE or LASLE significantly increased the localization of BMV-1a–mC at the perinuclear ER membrane, increasing the percentage of *erv14Δ* cells with a ring structure from 15% to 32% or 42%, respectively (Fig. 5B). Inclusion of the linker, however, did not have a significant effect (Fig. 5A,B).

Given that receptor-dependent cargos have been shown to weakly bind Sec24, the failed ER exit of cargos can be rescued by overexpressing Sec24 in cells lacking the cargo receptor. For example, overexpression of Sec24 promotes ER exit of yeast oligomycin resistance 1 (Yor1), an Erv14-dependent cargo, in *erv14Δ* cells (Pagant et al., 2015). We found that in ~44% of *erv14Δ* cells, BMV-1a–mC properly localized to the perinuclear ER when Sec24 was overexpressed, in sharp contrast to ~15% of cells expressing an empty vector (Fig. 5C). This result supports a role for Sec24 in targeting BMV 1a to the perinuclear ER along with Erv14.

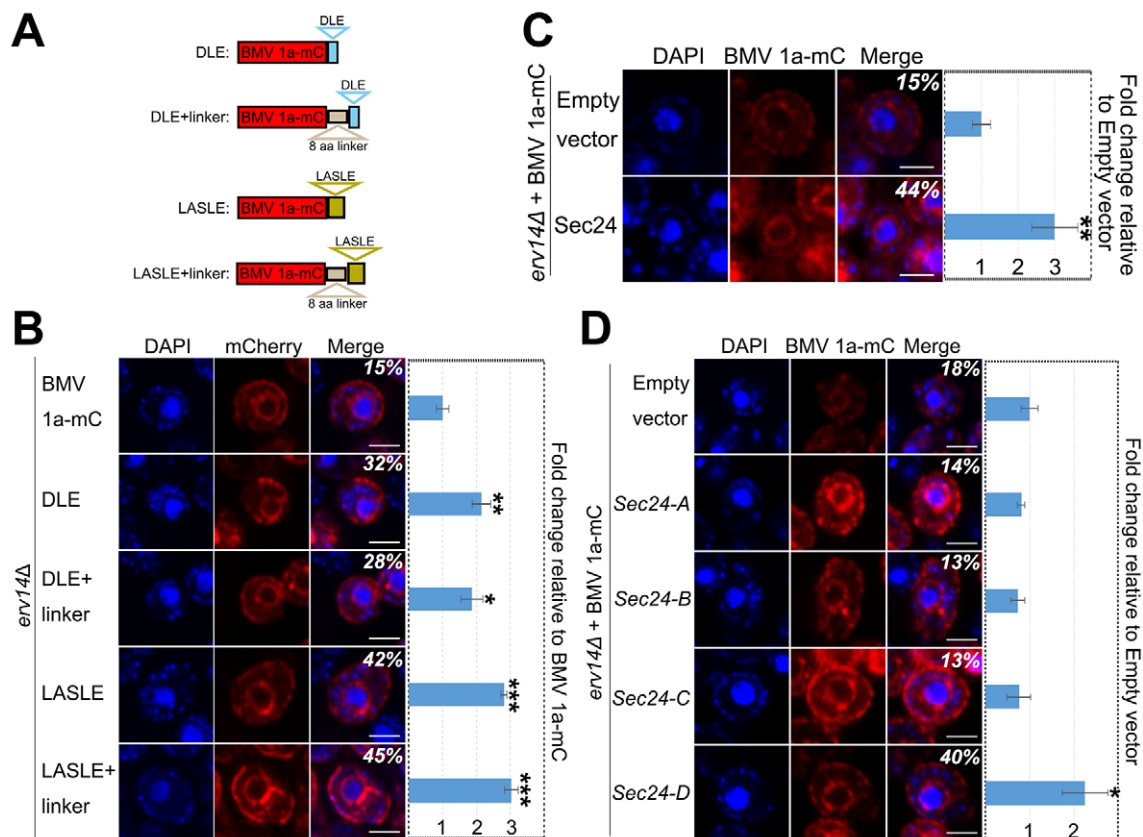


Fig. 5. Sec24 is involved in targeting BMV-1a–mC to the perinuclear ER membrane. (A) Diagram of various BMV-1a–mC derivatives fused to a DLE or LASLE sorting signal. An 8-amino-acid linker (GDGAGLIN) was inserted between BMV-1a–mC and DLE or LASLE in two vectors. (B–D) Percentage of cells showing the ring pattern in *erv14Δ* cells expressing BMV-1a–mC ($n=1119$), BMV-1a–mC–DLE ($n=1152$), –DLE+linker ($n=988$), –LASLE ($n=1059$), or –LASLE+linker ($n=962$) (B), empty vector ($n=1229$) or wt Sec24 ($n=1400$) (C), and empty vector ($n=1810$), Sec24-A ($n=1521$), Sec24-B ($n=1558$), Sec24-C ($n=1945$) or Sec24-D ($n=2093$) (D). Representative images of cells expressing with a ring pattern are shown. Results are mean \pm s.d. * $P<0.05$, ** $P<0.01$, *** $P<0.001$ (ANOVA single factor analysis as in Fig. 1). Scale bars: 2 μ m.

Sec24 has four binding sites that enable it to recognize various sorting signals present in different groups of cargos (Miller et al., 2003; Pagant et al., 2015). The A site recognizes the sorting signal YNNSNPF of Sed5, the B site binds to the sorting signal DxE or LASLE, the C site binds to Sec22, and the D site binds to Erv14 (Mossesova et al., 2003; Pagant et al., 2015). To examine which binding site(s) might play a crucial role in the perinuclear ER localization of BMV 1a, we overexpressed Sec24 with mutations in each site, denoted *Sec24-A*, *Sec24-B*, *Sec24-C* or *Sec24-D*. Overexpression of the *Sec24-D* mutant largely reversed the defective localization of BMV-1a-mC in *erv14Δ* cells (Fig. 5D). It should be noted that this result does not suggest that the D site is not important for BMV 1a distribution, rather, it is consistent with the fact that the Sec24 D site binds to Erv14 (Pagant et al., 2015). However, overexpressing the *Sec24-A*, *Sec24-B* or *Sec24-C* mutant did not improve BMV-1a-mC distribution in *erv14Δ* cells, suggesting that all three binding sites play an important role in the localization of BMV 1a and might be responsible for its proper localization in the 17% of *erv14Δ* cells with the ring pattern (Fig. 1).

COPII coat proteins are required for the perinuclear ER localization of BMV-1a-mC

Given that both Erv14 and Sec24 were involved in the perinuclear ER association of BMV-1a-mC, we wondered whether other COPII coat subunits were also involved in maintaining the normal distribution of BMV 1a. To this end, we checked BMV-1a-mC distribution in COPII temperature-sensitive (*ts*) strains of the four COPII coat subunits: *sec23-1*, *sec24*, *sec13-1* and *sec31-1*. We also tested a *ts* mutant of Sec12, which activates and recruits Sar1 to the ER to initiate the COPII vesicle assembly (D'Arcangelo et al., 2013; Lord et al., 2013). BMV-1a-mC was expressed in all *ts* mutants under both permissive (23°C) and restrictive temperatures (30 and 37°C) and its distribution was determined. Surprisingly, BMV-1a-mC was localized correctly at the perinuclear ER in *sec12-4* and *sec23-1*, even after the strains were incubated at non-permissive temperatures for 2 h (Fig. 6 for 37°C). To verify that these mutations completely blocked the function of these proteins (as would be expected due to their lethality at the restrictive temperature), we monitored ER exit of cell division cycle 50 (Cdc50), an Erv14-

dependent cargo (Herzig et al., 2012; Pagant et al., 2015). Although Cdc50-HA localized to the Golgi at 23°C in *sec23-1* cells, it was retained in ER membranes at 37°C (Fig. S3), indicating an inhibition of ER exit in the *sec23-1* mutant and confirming that Sec23 is not required for proper BMV 1a localization. Strikingly, BMV-1a-mC was mislocalized in more than 95% of *sec24* and *sec13-1* mutant cells incubated at 37°C for 2 h (Fig. 6). The distributions of BMV-1a-mC in these mutants, however, were different. In *sec24* cells there were one or two punctate dots, whereas larger aggregates were detected in *sec13-1* cells (Fig. 6A). In addition, in the *sec31-1* mutant, less than 30% of cells had a ring pattern ($P<0.01$, Fig. 6B). Collectively, these results suggest that Sec13, Sec24 and Sec31 are required for the proper localization of BMV-1a-mC.

Given that the C site in Sec24 binds to Sec22 and overexpressing *Sec24-C* failed to rescue the mis-localization phenotype for BMV-1a-mC in *erv14Δ* cells (Fig. 5D), Sec22 could also be involved in regulating the distribution of BMV 1a (Fig. 5D). Agreeing well with the result from the *Sec24-C* mutant, the ring pattern was observed in 35% of *sec22-3* cells when they were cultured at 37°C for 2 h, a significant reduction ($P<0.05$) from the 52% seen in wt cells.

The plant homologs of ERV14, Cornichons, complement the loss of Erv14 in yeast

Erv14 belongs to a conserved protein family called Cornichons (CNIs). CNIs are functionally conserved among eukaryotes, from yeast to *Drosophila* and mammals (Brandizzi and Barlowe, 2013; Dancourt and Barlowe, 2010). We first examined whether any plant CNIs could functionally complement the defective localization of BMV-1a-mC in *erv14Δ* cells. There are five CNI genes in *Arabidopsis thaliana*, referred to as CNI homologs (*AtCNIH*s): AT4G12090 (*AtCNIH1*), AT1G12340 (*AtCNIH2*), AT1G12390 (*AtCNIH3*), AT1G62880 (*AtCNIH4*), and AT3G12180 (*AtCNIH5*) (Rosas-Santiago et al., 2015). Each *AtCNIH* was expressed from a low-copy-number plasmid under the control of the *ERV14* endogenous promoter to achieve similar protein levels to endogenous Erv14. BMV-1a-mC was then expressed along with each *AtCNIH* in *erv14Δ* cells. We found that yeast expressing *AtCNIH1*, *AtCNIH4* and *AtCNIH5* had a similar percentage of cells

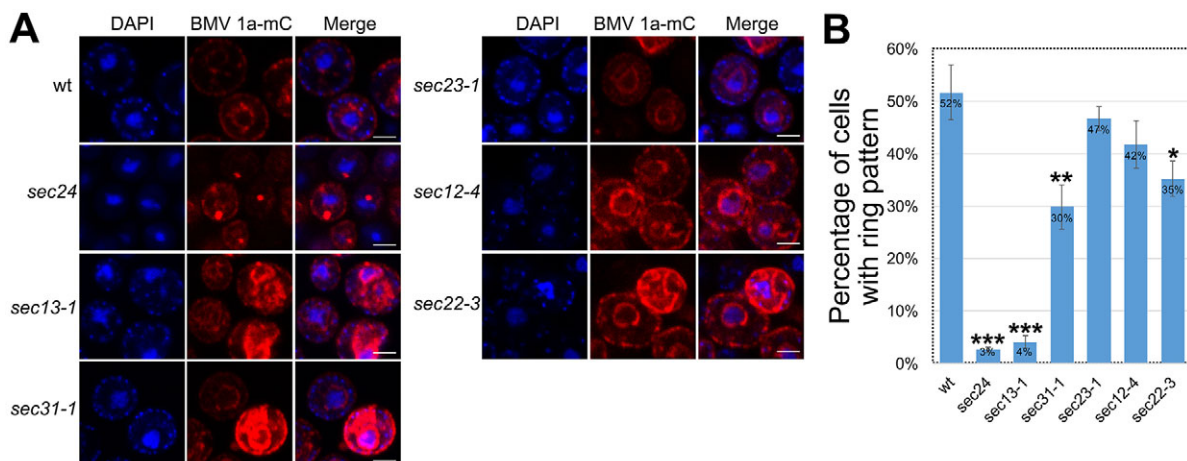


Fig. 6. Localization of BMV-1a-mC in mutants with dysfunctional COPII components. (A) Distribution of BMV-1a-mC in wt and COPII temperature-sensitive mutants after incubating cells at 37°C for 2 h. Representative images of the major localization patterns for BMV-1a-mC are shown. Scale bars: 2 μm. (B) Percentage of cells with a ring pattern in wt and each mutant after incubation at 37°C for 2 h. Total valid number of cells analyzed for each strain: wt ($n=746$), *sec24* ($n=919$), *sec13-1* ($n=1163$), *sec31-1* ($n=776$), *sec23-1* ($n=713$), *sec12-4* ($n=965$) and *sec22-3* ($n=842$). Results are mean±s.d. * $P<0.05$, ** $P<0.01$, *** $P<0.001$ (ANOVA single factor analysis as in Fig. 1).

with a ring pattern to those expressing wt *Erv14* (Fig. 7). In contrast, cells expressing *AtCNIH2* and *AtCNIH3* did not increase the percentage of cells with a ring pattern as compared to the empty plasmid (Fig. 7). We concluded that *AtCNIH1*, *AtCNIH4* and *AtCNIH5* are functionally equivalent to *Erv14* in yeast and suggest that they might contribute to BMV replication in plants.

DISCUSSION

All well-studied (+)RNA viruses target their replication proteins to organelle membranes or specific membrane microdomains to initiate VRC formation. Understanding the mechanisms by which viral proteins are targeted to particular organelle membranes will identify potential targets during the early steps of viral replication and offer insights into the development of novel antiviral strategies for virus control in humans, animals and crops.

Previous studies have demonstrated that host factors are crucial for intracellular membrane association of viral replication proteins in plants. Tomato mosaic virus (ToMV) encodes two replication proteins, the 130K helicase-like protein and the 180K replicase. Although both proteins do not have TMDs, a pool of these proteins is associated with host membranes in VRCs (Hagiwara et al., 2003; Ishibashi et al., 2012). The host integral membrane proteins tobamovirus multiplication 1 (TOM1) and TOM3 interact with ToMV replication proteins and serve as membrane anchors for ToMV VRCs (Ishikawa et al., 1993; Yamanaka et al., 2002, 2000).

Mutating both TOM1 and TOM3 completely inhibits ToMV infection (Yamanaka et al., 2002). By contrast, the viral protein 6 kDa protein 2 (6K₂) of tobacco etch virus (TEV) and turnip mosaic virus (TuMV) is responsible for initiating the assembly of 6K₂-induced vesicles (6K₂-vesicles). These vesicles serve as VRCs, exit ER membranes and eventually assemble into large granule structures at chloroplasts in addition to playing a possible role in cell-to-cell movement (Cheng et al., 2015; Cotton et al., 2009; Jiang et al., 2015; Wei and Wang, 2008; Wei et al., 2010). Out of the three *Arabidopsis* Sec24 isoforms (Sec24a, Sec24b and Sec24c) (Marti et al., 2010), 6K₂ interacts with Sec24a to assemble 6K₂-vesicles at ER exit sites (ERES). Indeed, the systemic spread of TuMV is reduced in a Sec24a-defective *Arabidopsis* mutant (Jiang et al., 2015), and a dominant-negative Sar1 mutant (H74L) blocks the formation of 6K₂ vesicles and virus spread (Wei and Wang, 2008). Coxsackievirus B3 (CVB3), a picornavirus, also assembles its VRCs at ERES and a dominant-negative Sar1 mutant (T39N) inhibits CVB3 replication by ~50% (Hsu et al., 2010). These data collectively indicate the importance of COPII vesicles in VRC formation for viruses in the picornavirus-like superfamily, which include CVB3, TEV and TuMV.

We report here that the perinuclear ER membrane association of BMV 1a is facilitated by the presence and canonical function of the cargo receptor *Erv14* (Figs 1 and 3). In support of *Erv14* acting as a canonical cargo receptor for BMV 1a is the fact that they physically interact (Fig. 4), that the ability of *Erv14* to bind cargo and to bind Sec24 is required for proper distribution of BMV-1a-mC (Fig. 3) and that the requirement of *Erv14* for distribution of BMV 1a was bypassed by addition of a Sec24-recognizable sorting signal to BMV-1a-mC or by overexpressing Sec24 (Fig. 5).

Our findings were surprising because BMV 1a is not a typical *Erv14*-dependent cargo as it lacks a long TMD. BMV 1a associates with ER membranes through an amphipathic α -helix (Liu et al., 2009). In contrast to the cargos that depend on COPII vesicles for ER exit, BMV 1a remains at the perinuclear ER and resides in the interior of spherules as a shell (Schwartz et al., 2002). BMV 1a is also not a typical Sec24-dependent cargo. For instance, overexpression of Sec24, or *Sec24-A*, *Sec24-C* or *Sec24-D* mutants, but not the *Sec24-B* mutant, support the exit of Yor1 from the ER in the absence of *Erv14*, as Yor1 has a sorting signal that weakly interacts with the Sec24 B site. However, with regards to perinuclear localization of BMV 1a, mutations in the Sec24 A, B or C site inhibited the ability of Sec24 to compensate for the absence of *ERV14*, suggesting that BMV 1a might bind to multiple sites within Sec24. Given that a mutated version of Sec24 (the *sec24 ts* mutant) altered BMV-1a-mC localization from the perinuclear ER membrane to dotted structures in 97% of cells, it indicates that Sec24 plays an active role in targeting BMV 1a to the perinuclear ER (Fig. 6).

How are *Erv14* and Sec24 involved in the perinuclear ER association of BMV 1a? As *Erv14* primarily localizes at the perinuclear ER membrane, one possibility is that BMV 1a is distributed to the perinuclear ER through its interaction with *Erv14* (Fig. 4). However, it should be noted that the interaction between BMV 1a and *Erv14* is either weak or transient because we could only pull them down together when cells were treated with formaldehyde to crosslink protein complexes (Fig. 4E). In addition, we can not totally rule out the possibility that BMV 1a interacts with *Erv14* through a protein that binds both and serves as a bridge. Similar to other *Erv14*-dependent client cargos, BMV 1a requires both *Erv14* and Sec24 for its targeting. One possibility is that *Erv14* and Sec24 recycle BMV 1a from peripheral tubular ER to

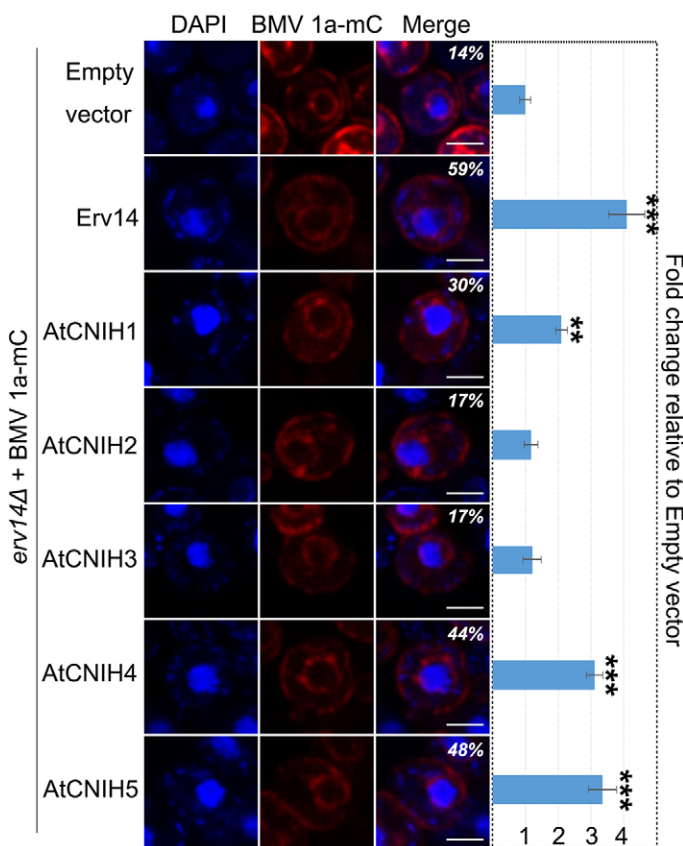


Fig. 7. Plant CNIs, homologs of *Erv14*, complement the loss of *ERV14* in yeast. Percentage of cells showing a ring pattern in *erv14Δ* cells co-expressing BMV-1a-mC with an empty vector ($n=842$), *Erv14* ($n=1122$), *AtCNIH1* ($n=1023$), *AtCNIH2* ($n=814$), *AtCNIH3* ($n=1252$), *AtCNIH4* ($n=1168$) or *AtCNIH5* ($n=965$). Representative images are shown. Results are mean \pm s.d. ** $P<0.01$, *** $P<0.001$ (ANOVA single factor analysis as in Fig. 1). Scale bars: 2 μ m.

the perinuclear regions. In support of this notion is the finding that a large pool of BMV-1a-mC dot and cluster structures colocalized with an ER marker in *erv14Δ* cells (Fig. 1D). This is also consistent with the fact that BMV 1a redistributes host reticulons from peripheral ER to the perinuclear ER through a direct interaction between BMV 1a and reticulons (Diaz et al., 2010). It is therefore possible that BMV 1a encounters reticulons at the peripheral ER tubules and redirects them to the perinuclear ER. It is also possible that BMV 1a remains at the perinuclear ER by interfering with the function of COPII vesicles for targeting itself out of the ER. However, our results are not consistent with this possibility, as the dot and cluster structures observed in *erv14Δ* cells colocalize with an ER marker (Fig. 1D) but not a Golgi marker (Fig. S2). Moreover, we cannot rule out the possibility that Erv14 and Sec24 might recruit BMV 1a into COPII vesicles to enrich and facilitate the self-interaction of BMV 1a. Several host proteins, including reticulons, Snf7 and Cho2, are recruited to spherules by BMV 1a and are required for the formation of functional VRCs (Diaz et al., 2010, 2015; Zhang et al., 2016). Given that spherule diameter increased, whereas the number of spherules per cell decreased, in *erv14Δ* cells (Fig. 2), it is also likely that Erv14 and/or Sec24 participates in forming or stabilizing spherules through their connection with BMV 1a. However, this awaits further evidence.

Although Sec13 is necessary for the proper localization of BMV-1a-mC, the possible role of Sec13 is less clear. As a NPC component, Sec13 is additionally localized to perinuclear ER membranes, besides residing in ERES. It should also be noted that eight hits in our screen are NPC components (Table 1). It is, therefore, possible that Erv14, Sec24 and Sec13 could target or maintain BMV 1a at the perinuclear ER by delivering BMV 1a to NPCs to initiate spherule formation.

Erv14 belongs to the conserved CNI family. CNIs have been well-studied in *Drosophila* and mammalian cells (Dancourt and Barlowe, 2010). CNI was first identified in *Drosophila* and is required for the transport of Gurken (Grk), a transforming growth factor α (TGF α), from the ER to the oocyte surface (Roth et al., 1995). Among four CNI homologs (CNIHs) in mammals, CNIH2 and CNIH3 function as α -amino-3-hydroxy-5-methyl-4-isoxazole-propionic acid (AMPA) receptors for glutamatergic neurotransmission in the central nervous system (Herring et al., 2013; Jackson and Nicoll, 2009; Schwenk et al., 2009). CNIH4 interacts with both G-protein-coupled receptors (GPCRs) and Sec23 and Sec24 and, thus, acts as a cargo receptor for recruiting GPCRs into COPII vesicles and transporting them to the cell surface (Sauvageau et al., 2014). Additionally, human CNIs functionally complement the loss of Erv14 in yeast (Castro et al., 2007). However, plant CNIs have not been well-studied. Recently, a specific rice CNI has been identified as a possible cargo receptor for the sodium transporter HKT1;3 to the Golgi (Rosas-Santiago et al., 2015). Among five CNI members in *Arabidopsis*, we showed that AtCNIH1, AtCNIH4 and AtCNIH5 are functionally equivalent to Erv14 in yeast (Fig. 7). The roles that AtCNIHs play in BMV replication in plants, however, are under further investigation.

In conclusion, we identified the cargo receptor Erv14 as a new host factor required for targeting BMV replication protein 1a to the perinuclear ER membrane, for VRC formation and genomic RNA replication. Our data are consistent with a working model that Erv14, through a direct interaction with BMV 1a, targets BMV 1a from ER membranes to, or maintains BMV 1a at, the perinuclear ER membrane, along with the COPII coat components Sec24, Sec13 and Sec31. Although COPII vesicles are known for their role in

anterograde protein transport from the ER to the Golgi and biogenesis of autophagosomes, our data suggest a new role for Erv14, Sec24, Sec13 and Sec31 in targeting or maintaining protein(s) at the perinuclear ER membrane.

MATERIALS AND METHODS

High-throughput yeast GFP-tagged library screening

Plasmid pB1YT3-mC, which expresses BMV-1a-mCherry, was transformed into an synthetic genetic array (SGA) compatible yeast strain (YMS140) and introduced into the yeast GFP-tagged library (Huh et al., 2003) using automated mating approaches (Cohen and Schuldiner, 2011; Herzig et al., 2012). The strains were imaged using a high-content screening platform (Breker et al., 2013) and the localization of all the GFP-tagged host proteins and BMV-1a-mC was analyzed by eye for colocalization.

Yeast strains and cell growth

Yeast strain YPH500 and its various single gene deletion derivatives were used in all experiments, unless specified otherwise. Temperature sensitive strains *sec12-4*, *sec13-1*, *sec22-3*, *sec23-1*, *sec31-1* and *sec24* were based on X2180-1A (Novick et al., 1980) or BY4741 (Li et al., 2011). All yeast cells were grown at 30°C, with the exception of *ts* strains, which were grown overnight at 23°C and sub-cultured for 2 h at 30°C or 37°C. All yeast cells were grown in defined synthetic medium containing 2% galactose as a carbon source. Leucine, uracil, histidine or combinations thereof were omitted to maintain plasmid selection. Cells were grown in galactose medium for two passages (36 to 48 h) and harvested when the optical density at 600 nm (OD_{600}) was between 0.4 and 1.0.

Plasmids, plasmid construction, and yeast transformation

His6-, mCherry- or HA-tagged versions of BMV 1a were expressed from pB1YT3-cH6, -mC, or -HA, respectively. BMV 1a and 2a^{pol} were expressed from pB12VG1 (Kushner et al., 2003) whereas BMV RNA3 was transcribed from pB3VG128-H (Zhang et al., 2012) to launch BMV replication in yeast cells. pB1YT3-mC was used as the vector to add the COPII recognizable sorting signal DLE or LASLE (Mossesso et al., 2003; Votsmeier and Gallwitz, 2001) to the C-terminus of BMV-1a-mC by overlapping PCR. For some constructs, a linker (GDGAGLIN) was added in between BMV-1a-mC and the sorting signal. GFP-tagged Scs2 served as an ER membrane marker, GFP-tagged Pmr1 served as a Golgi marker, and GFP-tagged VHL served as an inclusion body marker. HA-tagged Erv14 mutants or *Arabidopsis* CNIHs (AtCNIHs) were expressed under the control of the *ERV14* endogenous promoter from a low-copy-number plasmid. For the mbSUS assay, target genes were either cloned into the bait vector pMetYCGate or the prey vectors pNXgate33-3HA or pXNgate21-3HA (Obrdlik et al., 2004).

Immunofluorescence confocal microscopy and proximity ligation assay

Two OD_{600} units of yeast cells were harvested and fixed with 4% (v/v) formaldehyde, and the cell wall was removed by lyticase treatment at 30°C for 1 h and permeabilized with 0.1% Triton X-100 for 15 min at room temperature. Spheroplasts were incubated with primary anti-HA pAb (Invitrogen, Cat. no. 71-5500, Lot no. 1544744A), anti-1a antiserum (Restrepo-Hartwig and Ahlquist, 1996), anti-His mAb (GeneScript, Cat. no. A00186, Lot no. 12L000548) or anti-Dpml mAb (Invitrogen, Cat. no. A6429, Lot no. 425998) at a 1:100 dilution overnight at 4°C, followed by a secondary antibody at 1:100 dilution for 1 h at 37°C. The secondary antibodies were anti-rabbit IgG conjugated to Alexa Fluor 488 or Alexa Fluor 594 (Jackson ImmunoResearch; Cat. no. 711-545-152, Lot no. 116141 or 711-585-152, Lot no. 113078, respectively) or anti-mouse IgG conjugated to Alexa Fluor 594 or Alexa Fluor 488 (Life Technologies; Cat. no. A11020, Lot no. 1606260 or A11001, Lot no. 1397999, respectively) at 1:100 dilution. The nucleus was stained with DAPI for 10 min and samples were observed using a Zeiss LSM Scanning 880 microscope or a Zeiss epifluorescence microscope (Observer.Z1) at the Fralin microscopy facility at Virginia Tech.

PLA was performed following the standard procedure (Duolink, Sigma). Briefly, yeast spheroplasts were incubated with anti-His mAb and anti-HA pAb or anti-Dpm1 mAb and anti-1a antiserum at 1:100 dilution overnight at 4°C, followed by a 1 h incubation at 37°C with antibodies conjugated to oligonucleotides (PLA probe Minus and Plus). After a 30-min ligation reaction and 100-min amplification reaction at 37°C, samples were stained with DAPI and observed using a Zeiss LSM Scanning 880 microscope.

Electron microscopy

Fixation, dehydration and embedding of yeast cells were performed as previously described (Zhang et al., 2012). Images were obtained using a JEOL JEM 1400 transmission electron microscope located at the Virginia-Maryland College of Veterinary Medicine, Virginia Tech.

RNA extraction and northern blotting

Total RNA was extracted from yeast cells that were harvested at OD₆₀₀ values of 0.4 to 1.0 by a hot phenol approach (Kohrer and Domdey, 1991). Northern blotting was performed as previously described (Zhang et al., 2012). Briefly, equal amounts of total RNA were separated by agarose-formaldehyde electrophoresis and transferred to Nytran membranes. BMV-positive- and negative-strand RNAs were detected using P³²-labeled probes specific to BMV RNAs. To eliminate loading variations, an 18S rRNA specific probe was used to normalize the signals. Radioactive signals were scanned by using a Typhoon FLA 7000 phosphorimager and the intensity of radioactive signals were quantified by using ImageQuant TL (GE healthcare).

Protein extraction and western blotting

Total proteins were extracted and western blotting was performed as described previously (Zhang et al., 2012). Briefly, two OD₆₀₀ units of yeast cells were harvested, broken in yeast lysis buffer (50 mM Tris-HCl pH 8.0, 10 mM MgCl₂, 1 mM EGTA, 2 mM EDTA pH 8, 20% Glycerol, and 15 mM KCl) containing a proteinase inhibitor mix (Sigma-Aldrich) at a 1:200 dilution using a bead beater. SDS lysis buffer (2% SDS, 90 mM Hepes, pH 7.5, 30 mM DTT) and loading buffer was added to the mixture and boiled for 5 min, the cell debris was removed and equal volumes of total protein extracts were loaded onto a 10% (v/v) SDS-PAGE gel, followed by the transfer of proteins to a polyvinylidene difluoride (PVDF) membrane. The membranes were incubated in anti-BMV 1a antiserum (1:10,000 dilution), anti-HA pAb (1:3000 dilution) or anti-Pgk1 mAb (1:10,000 dilution, Invitrogen, Cat. no. 459250, Lot no. C0240) primary antibodies, followed by anti-rabbit-IgG or anti-mouse-IgG secondary antibodies conjugated to horseradish peroxidase (HRP) (Thermo Scientific, Cat no. 32460, Lot no. LH148799 or 32430, Lot no. LK152904) at 1:10,000 dilution. The membranes were incubated in Supersignal West Femto substrate (Thermo Scientific) and the protein signals were detecting using X-ray film or a Bio-Rad ChemiDoc imager.

Chemical crosslinking and co-immunoprecipitation assay

Ten OD₆₀₀ units of yeast cells were harvested, resuspended in 5 ml of growth medium containing 1% formaldehyde, incubated at 30°C for 10 min and quenched at 30°C for 10 min by adding glycine at a final concentration of 0.125 M. The co-immunoprecipitation assay was performed as previously described (Diaz et al., 2010). Briefly, crosslinked cells were lysed in RIPA buffer (50 mM Tris-HCl pH 8.0, 1% Nonidet P-40, 0.1% SDS, 150 mM NaCl, 0.5% sodium deoxycholate, 5 mM EDTA, 10 mM NaF, 10 mM NaPPI, and protease inhibitor mix) by glass beads in a bead beater for 2 min and further incubated in RIPA buffer at 4°C for 2 h. Cell debris was removed and the supernatant was mixed with Protein-A-sepharose beads (GE Healthcare) and anti-His mAb overnight at 4°C. Beads were washed three times with RIPA buffer, re-suspended in 1× SDS loading buffer and incubated at 50°C for 20 min to release the proteins. Samples were boiled for 10 min before being loaded onto a 10% (v/v) SDS-PAGE gel, followed by western blotting to detect target proteins using anti-HA pAb.

Statistical analysis of BMV 1a localization pattern

The percentage of cells with ring, dot and cluster localization patterns of BMV 1a was calculated based on the total number of cells that had a visible

nucleus as well as a BMV-1a-mC signal. The numbers of cells counted for each assay are shown in the figure legends. Each experiment was repeated at least three times and the percentages shown in the figures represent the average of all the experiments. The formula for calculating the percentage of cells with the ring localization is as following: number of cells with the ring pattern/(number of cells with ring+number of cells with dot+number of cells with cluster). A similar formula was used to calculate percentages of cells with dot or cluster patterns. ANOVA single factor analysis was used to test percentage of cells with BMV-1a-mC ring localization pattern in comparison to that in negative control. Error bars represents the standard deviation.

Acknowledgements

We thank Drs Elizabeth Miller at the MRC Laboratory of Molecular Biology, UK, Randy Schekman at University of California-Berkeley, and Charles Boone at the University of Toronto for providing plasmids and yeast mutant strains. We also want to thank Drs Arturo Diaz and Janet Webster for critical reading of the manuscript. We thank Dr Kristi DeCourcy at the confocal microscopy facility in the Fralin Life Science Institute and Ms. Kathy Lowe at the electron microscopy facility at the Virginia-Maryland College of Veterinary Medicine, Virginia Tech for imaging assistance.

Competing interests

The authors declare no competing or financial interests.

Author contributions

X.W., J.L. and M.S. conceived and designed the experiments; J.L., S.F. and J.Z. performed the experiments; J.L. and S.F. analyzed data; X.W., J.L. and M.S. wrote the manuscript; and X.W. coordinated the study.

Funding

This work was supported by an US-Israel Binational Science Foundation (BSF) collaborative grant [grant number 2013101 to Elizabeth Miller (MRC Laboratory of Molecular Biology, Cambridge, UK) and M.S.]; and a Virginia Tech Startup and a National Science Foundation (NSF) grant [grant number 1265260 to X.W.].

Supplementary information

Supplementary information available online at <http://jcs.biologists.org/lookup/doi/10.1242/jcs.190082.supplemental>

References

- Ahola, T. and Ahlquist, P. (1999). Putative RNA capping activities encoded by bromo mosaic virus: methylation and covalent binding of guanylate by replicase protein 1a. *J. Virol.* **73**, 10061–10069.
- Antebi, A. and Fink, G. R. (1992). The yeast Ca(2+)-ATPase homologue, PMR1, is required for normal Golgi function and localizes in a novel Golgi-like distribution. *Mol. Biol. Cell* **3**, 633–654.
- Belden, W. J. and Barlowe, C. (2001). Role of Erv29p in collecting soluble secretory proteins into ER-derived transport vesicles. *Science* **294**, 1528–1531.
- Boone, C., Sdicu, A., Laroche, M. and Bussey, H. (1991). Isolation from *Candida albicans* of a functional homolog of the *Saccharomyces cerevisiae* KRE1 gene, which is involved in cell wall beta-glucan synthesis. *J. Bacteriol.* **173**, 6859–6864.
- Brandizzi, F. and Barlowe, C. (2013). Organization of the ER-Golgi interface for membrane traffic control. *Nat. Rev. Mol. Cell Biol.* **14**, 382–392.
- Brandizzi, F. and Barlowe, C. (2014). ER-Golgi transport: authors' response. *Nat. Rev. Mol. Cell Biol.* **15**, 1.
- Breker, M., Gymrek, M. and Schuldiner, M. (2013). A novel single-cell screening platform reveals proteome plasticity during yeast stress responses. *J. Cell Biol.* **200**, 839–850.
- Castro, C. P., Piscopo, D., Nakagawa, T. and Derynck, R. (2007). Cornichon regulates transport and secretion of TGF α -related proteins in metazoan cells. *J. Cell Sci.* **120**, 2454–2466.
- Cheng, X., Deng, P., Cui, H. and Wang, A. (2015). Visualizing double-stranded RNA distribution and dynamics in living cells by dsRNA binding-dependent fluorescence complementation. *Virology* **485**, 439–451.
- Cohen, Y. and Schuldiner, M. (2011). Advanced methods for high-throughput microscopy screening of genetically modified yeast libraries. In *Netw Biol*, Vol. 781 (ed. G. Cagny and A. Emili), pp. 127–159: Humana Press.
- Cotton, S., Grangeon, R., Thivierge, K., Mathieu, I., Ide, C., Wei, T., Wang, A. and Laliberté, J.-F. (2009). Turnip mosaic virus RNA replication complex vesicles are mobile, align with microfilaments, and are each derived from a single viral genome. *J. Virol.* **83**, 10460–10471.
- Dancourt, J. and Barlowe, C. (2010). Protein sorting receptors in the early secretory pathway. *Annu. Rev. Biochem.* **79**, 777–802.

- D'Arcangelo, J. G., Stahmer, K. R. and Miller, E. A. (2013). Vesicle-mediated export from the ER: COPII coat function and regulation. *Biochim. Biophys. Acta* **1833**, 2464-2472.
- Davis, S. and Ferro-Novick, S. (2015). Ypt1 and COPII vesicles act in autophagosome biogenesis and the early secretory pathway. *Biochem. Soc. Trans.* **43**, 92-96.
- den Boon, J. A., Diaz, A. and Ahlquist, P. (2010). Cytoplasmic viral replication complexes. *Cell Host Microbe* **8**, 77-85.
- Diaz, A. and Wang, X. (2014). Bromovirus-induced remodeling of host membranes during viral RNA replication. *Curr. Opin. Virol.* **9**, 104-110.
- Diaz, A., Wang, X. and Ahlquist, P. (2010). Membrane-shaping host reticulon proteins play crucial roles in viral RNA replication compartment formation and function. *Proc. Natl. Acad. Sci. USA* **107**, 16291-16296.
- Diaz, A., Gallei, A. and Ahlquist, P. (2012). Bromovirus RNA replication compartment formation requires concerted action of 1a's self-interacting RNA capping and helicase domains. *J. Virol.* **86**, 821-834.
- Diaz, A., Zhang, J., Ollwerther, A., Wang, X. and Ahlquist, P. (2015). Host ESCRT proteins are required for bromovirus RNA replication compartment assembly and function. *PLoS Pathog.* **11**, e1004742.
- Ge, L., Zhang, M. and Schekman, R. (2014). Phosphatidylinositol 3-kinase and COPII generate LC3 lipidation vesicles from the ER-Golgi intermediate compartment. *Elife* **3**, e04135.
- Hagiwara, Y., Komoda, K., Yamanaka, T., Tamai, A., Meshi, T., Funada, R., Tsuchiya, T., Naito, S. and Ishikawa, M. (2003). Subcellular localization of host and viral proteins associated with tobamovirus RNA replication. *EMBO J.* **22**, 344-353.
- Herring, B. E., Shi, Y., Suh, Y. H., Zheng, C.-Y., Blankenship, S. M., Roche, K. W. and Nicoll, R. A. (2013). Cornichon proteins determine the subunit composition of synaptic AMPA receptors. *Neuron* **77**, 1083-1096.
- Herzig, Y., Sharpe, H. J., Elbaz, Y., Munro, S. and Schuldiner, M. (2012). A systematic approach to pair secretory cargo receptors with their cargo suggests a mechanism for cargo selection by Erv14. *PLoS Biol.* **10**, e1001329.
- Hsu, N.-Y., Ilnytska, O., Belov, G., Santiana, M., Chen, Y.-H., Takvorian, P. M., Pau, C., van der Schaar, H., Kaushik-Basu, N., Balla, T. et al. (2010). Viral reorganization of the secretory pathway generates distinct organelles for RNA replication. *Cell* **141**, 799-811.
- Huh, W.-K., Falvo, J. V., Gerke, L. C., Carroll, A. S., Howson, R. W., Weissman, J. S. and O'Shea, E. K. (2003). Global analysis of protein localization in budding yeast. *Nature* **425**, 686-691.
- Ishibashi, K., Miyashita, S., Katoh, E. and Ishikawa, M. (2012). Host membrane proteins involved in the replication of tobamovirus RNA. *Curr. Opin. Virol.* **2**, 699-704.
- Ishikawa, M., Naito, S. and Ohno, T. (1993). Effects of the tom1 mutation of *Arabidopsis thaliana* on the multiplication of tobacco mosaic virus RNA in protoplasts. *J. Virol.* **67**, 5328-5338.
- Jackson, A. C. and Nicoll, R. A. (2009). Neuroscience: AMPA receptors get 'pickled'. *Nature* **458**, 585-586.
- Janda, M. and Ahlquist, P. (1993). RNA-dependent replication, transcription, and persistence of brome mosaic virus RNA replicons in *S. cerevisiae*. *Cell* **72**, 961-970.
- Jiang, J., Patarroyo, C., Garcia Cabanillas, D., Zheng, H. and Laliberté, J.-F. (2015). The vesicle-forming 6K2 protein of turnip mosaic virus interacts with the COPII coatomer Sec24a for viral systemic infection. *J. Virol.* **89**, 6695-6710.
- Kaganovich, D., Kopito, R. and Frydman, J. (2008). Misfolded proteins partition between two distinct quality control compartments. *Nature* **454**, 1088-1095.
- Kohrer, K. and Domdey, H. (1991). Preparation of high molecular weight RNA. *Methods Enzymol.* **194**, 398-405.
- Kong, F., Sivakumaran, K. and Kao, C. (1999). The N-terminal half of the brome mosaic virus 1a protein has RNA capping-associated activities: specificity for GTP and s-adenosylmethionine. *Virology* **259**, 200-210.
- Kuehn, M. J., Herrmann, J. M. and Schekman, R. (1998). COPII-cargo interactions direct protein sorting into ER-derived transport vesicles. *Nature* **391**, 187-190.
- Kushner, D. B., Lindenbach, B. D., Grdzelskivili, V. Z., Noueiry, A. O., Paul, S. M. and Ahlquist, P. (2003). Systematic, genome-wide identification of host genes affecting replication of a positive-strand RNA virus. *Proc. Natl. Acad. Sci. USA* **100**, 15764-15769.
- Laliberté, J.-F. and Sanfaçon, H. (2010). Cellular remodeling during plant virus infection. *Annu. Rev. Phytopathol.* **48**, 69-91.
- Li, Z., Vizeacoumar, F. J., Bahr, S., Li, J., Warringer, J., Vizeacoumar, F. S., Min, R., VanderSluis, B., Bellay, J., DeVit, M. et al. (2011). Systematic exploration of essential yeast gene function with temperature-sensitive mutants. *Nat. Biotech.* **29**, 361-367.
- Liu, L., Westler, W. M., Den Boon, J. A., Wang, X., Diaz, A., Steinberg, H. A. and Ahlquist, P. (2009). An amphipathic α -helix controls multiple roles of brome mosaic virus protein 1a in RNA replication complex assembly and function. *PLoS Pathog.* **5**, e1000351.
- Lord, C., Ferro-Novick, S. and Miller, E. A. (2013). The highly conserved COPII coat complex sorts cargo from the endoplasmic reticulum and targets it to the golgi. *Cold Spring Harb. Perspect. Biol.* **5**, pii: a013367.
- Manford, A. G., Stefan, C. J., Yuan, H. L., MacGurn, J. A. and Emr, S. D. (2012). ER-to-plasma membrane tethering proteins regulate cell signaling and ER morphology. *Dev. Cell* **23**, 1129-1140.
- Marti, L., Fornaciari, S., Renna, L., Stefano, G. and Brandizzi, F. (2010). COPII-mediated traffic in plants. *Trends Plant Sci.* **15**, 522-528.
- Miller, E. A., Beilharz, T. H., Malkus, P. N., Lee, M. C. S., Hamamoto, S., Orci, L. and Schekman, R. (2003). Multiple cargo binding sites on the COPII subunit Sec24p ensure capture of diverse membrane proteins into transport vesicles. *Cell* **114**, 497-509.
- Mo, C. and Bard, M. (2005). A systematic study of yeast sterol biosynthetic protein-protein interactions using the split-ubiquitin system. *Biochim. Biophys. Acta Mol. Cell Biol.* **1737**, 152-160.
- Mossessova, E., Bickford, L. C. and Goldberg, J. (2003). SNARE selectivity of the COPII coat. *Cell* **114**, 483-495.
- Novick, P., Field, C. and Schekman, R. (1980). Identification of 23 complementation groups required for post-translational events in the yeast secretory pathway. *Cell* **21**, 205-215.
- Obdrlik, P., El-Bakkoury, M., Hamacher, T., Cappellaro, C., Vilarino, C., Fleischer, C., Ellerbrok, H., Kamuzinzi, R., Ledent, V., Blaudez, D. et al. (2004). K⁺ channel interactions detected by a genetic system optimized for systematic studies of membrane protein interactions. *Proc. Natl. Acad. Sci. USA* **101**, 12242-12247.
- O'Reilly, E. K., Paul, J. D. and Kao, C. C. (1997). Analysis of the interaction of viral RNA replication proteins by using the yeast two-hybrid assay. *J. Virol.* **71**, 7526-7532.
- Pagant, S., Wu, A., Edwards, S., Diehl, F. and Miller, E. A. (2015). Sec24 is a coincidence detector that simultaneously binds two signals to drive ER export. *Curr. Biol.* **25**, 403-412.
- Paul, D. and Bartschlagler, R. (2013). Architecture and biogenesis of plus-strand RNA virus replication factories. *World J. Virol.* **2**, 32-48.
- Powers, J. and Barlowe, C. (2002). Erv14p directs a transmembrane secretory protein into COPII-coated transport vesicles. *Mol. Biol. Cell* **13**, 880-891.
- Restrepo-Hartwig, M. A. and Ahlquist, P. (1996). Brome mosaic virus helicase- and polymerase-like proteins colocalize on the endoplasmic reticulum at sites of viral RNA synthesis. *J. Virol.* **70**, 8908-8916.
- Romero-Brey, I. and Bartschlagler, R. (2014). Membranous replication factories induced by plus-strand RNA viruses. *Virology* **6**, 2826-2857.
- Rosas-Santiago, P., Lagunas-Gómez, D., Barkla, B. J., Vera-Estrella, R., Lalonde, S., Jones, A., Frommer, W. B., Zimmermannova, O., Sychrová, H. and Pantoja, O. (2015). Identification of rice cornichon as a possible cargo receptor for the Golgi-localized sodium transporter OsHKT1;3. *J. Exp. Bot.* **66**, 2733-2748.
- Roth, S., Shira Neuman-Silberberg, F., Barcelo, G. and Schüpbach, T. (1995). *cornichon* and the EGF receptor signaling process are necessary for both anterior-posterior and dorsal-ventral pattern formation in *Drosophila*. *Cell* **81**, 967-978.
- Sauvageau, E., Rochdi, M. D., Oueslati, M., Hamdan, F. F., Percherancier, Y., Simpson, J. C., Pepperkok, R. and Bouvier, M. (2014). CNH4 interacts with newly synthesized GPCR and controls their export from the endoplasmic reticulum. *Traffic* **15**, 383-400.
- Schwartz, M., Chen, J., Janda, M., Sullivan, M., den Boon, J. and Ahlquist, P. (2002). A positive-strand RNA virus replication complex parallels form and function of retrovirus capsids. *Mol. Cell* **9**, 505-514.
- Schwenk, J., Harmel, N., Zolles, G., Bildl, W., Kulik, A., Heimrich, B., Chisaka, O., Jonas, P., Schulte, U., Fakler, B. et al. (2009). Functional proteomics identify cornichon proteins as auxiliary subunits of AMPA receptors. *Science* **323**, 1313-1319.
- Soderberg, O., Gullberg, M., Jarvius, M., Ridderstrale, K., Leuchowius, K.-J., Jarvius, J., Wester, K., Hydbring, P., Bahram, F., Larsson, L.-G. et al. (2006). Direct observation of individual endogenous protein complexes in situ by proximity ligation. *Nat. Methods* **3**, 995-1000.
- Taron, C. H., Wiedman, J. M., Grimme, S. J. and Orlean, P. (2000). Glycosylphosphatidylinositol biosynthesis defects in Gpi11p- and Gpi13p-deficient yeast suggest a branched pathway and implicate Gpi13p in phosphoethanolamine transfer to the third mannose. *Mol. Biol. Cell* **11**, 1611-1630.
- Votsmeier, C. and Gallwitz, D. (2001). An acidic sequence of a putative yeast Golgi membrane protein binds COPII and facilitates ER export. *EMBO J.* **20**, 6742-6750.
- Wang, X. and Ahlquist, P. (2008). Brome mosaic virus (Bromoviridae). In *Encyclopedia of Virology*, 3rd edn. (ed. B. W. J. Mahy and M. H. V. van Regenmortel), pp. 381-386. Boston: Academic Press.
- Wang, X., Lee, W.-M., Watanabe, T., Schwartz, M., Janda, M. and Ahlquist, P. (2005). Brome mosaic virus 1a nucleoside triphosphatase/helicase domain plays crucial roles in recruiting RNA replication templates. *J. Virol.* **79**, 13747-13758.
- Wang, J., Tan, D., Cai, Y., Reinisch, K. M., Walz, T. and Ferro-Novick, S. (2014). A requirement for ER-derived COPII vesicles in phagophore initiation. *Autophagy* **10**, 708-709.
- Wei, T. and Wang, A. (2008). Biogenesis of cytoplasmic membranous vesicles for plant potyvirus replication occurs at endoplasmic reticulum exit sites in a COPI- and COPII-dependent manner. *J. Virol.* **82**, 12252-12264.

- Wei, T., Zhang, C., Hong, J., Xiong, R., Kasschau, K. D., Zhou, X., Carrington, J. C. and Wang, A.** (2010). Formation of complexes at plasmodesmata for Potyvirus intercellular movement is mediated by the viral protein P3N-PIPO. *PLoS Pathog.* **6**, e1000962.
- Yamanaka, T., Ohta, T., Takahashi, M., Meshi, T., Schmidt, R., Dean, C., Naito, S. and Ishikawa, M.** (2000). TOM1, an Arabidopsis gene required for efficient multiplication of a tobamovirus, encodes a putative transmembrane protein. *Proc. Natl. Acad. Sci. USA* **97**, 10107-10112.
- Yamanaka, T., Imai, T., Satoh, R., Kawashima, A., Takahashi, M., Tomita, K., Kubota, K., Meshi, T., Naito, S. and Ishikawa, M.** (2002). Complete inhibition of tobamovirus multiplication by simultaneous mutations in two homologous host genes. *J. Virol.* **76**, 2491-2497.
- Zhang, J., Diaz, A., Mao, L., Ahlquist, P. and Wang, X.** (2012). Host acyl coenzyme A binding protein regulates replication complex assembly and activity of a positive-strand RNA virus. *J. Virol.* **86**, 5110-5121.
- Zhang, J., Zhang, Z., Chukkapalli, V., Nchoutmboube, J. A., Li, J., Randall, G., Belov, G. A. and Wang, X.** (2016). Positive-strand RNA viruses stimulate host phosphatidylcholine synthesis at viral replication sites. *Proc. Natl. Acad. Sci. USA* **113**, E1064-E1073.